Title	Second-order data obtained from differential pulse voltammetry: Determination of tryptophan at a gold nanoparticles decorated multiwalled carbon nanotube modified glassy carbon electrode
Author(s)	Kooshki, Mojtaba; Abdollahi, Hamid; Bozorgzadeh, Somayyeh; Haghighi, Behzad
Publication date	2011-08-05
Original citation	Kooshki, M., Abdollahi, H., Bozorgzadeh, S. and Haghighi, B. (2011) 'Second-order data obtained from differential pulse voltammetry: Determination of tryptophan at a gold nanoparticles decorated multiwalled carbon nanotube modified glassy carbon electrode', Electrochimica Acta, 56 (24), pp. 8618-8624. doi: 10.1016/j.electacta.2011.07.049
Type of publication	Article (peer-reviewed)
Link to publisher's version	https://doi.org/10.1016/j.electacta.2011.07.049 http://dx.doi.org/10.1016/j.electacta.2011.07.049 Access to the full text of the published version may require a subscription.
Rights	© 2021 Elsevier Ltd. This manuscript version is made available under the CC-BY-NC-ND 4.0 license https://creativecommons.org/licenses/by-nc-nd/4.0/ https://creativecommons.org/licenses/by-nc-nd/4.0/
Item downloaded from	http://hdl.handle.net/10468/13518

University College Cork, Ireland
Coláiste na hOllscoile Corcaigh

Accepted Manuscript

Title: Second-order data obtained from differential pulse voltammetry: determination of tryptophan at a gold nanoparticles decorated multiwalled carbon nanotube modified glassy carbon electrode

Authors: Mojtaba Kooshki, Hamid Abdollahi, Somayyeh Bozorgzadeh, Behzad Haghighi
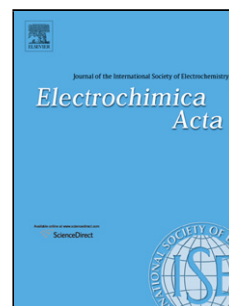
Please cite this article as: M. Kooshki, H. Abdollahi, S. Bozorgzadeh, B. Haghighi, Second-order data obtained from differential pulse voltammetry: determination of tryptophan at a gold nanoparticles decorated multiwalled carbon nanotube modified glassy carbon electrode, *Electrochimica Acta* (2010), doi:10.1016/j.electacta.2011.07.049

This is a PDF file of an unedited manuscript that has been accepted for publication. As a service to our customers we are providing this early version of the manuscript. The manuscript will undergo copyediting, typesetting, and review of the resulting proof before it is published in its final form. Please note that during the production process errors may be discovered which could affect the content, and all legal disclaimers that apply to the journal pertain.

Second-order data obtained from differential pulse voltammetry: determination of tryptophan at a gold nanoparticles decorated multiwalled carbon nanotube modified glassy carbon electrode

Mojtaba Kooshki, Hamid Abdollahi[*], Somayyeh Bozorgzadeh and Behzad Haghighi

Department of Chemistry, Institute for Advanced Studies in Basic Sciences, P.O. Box 45195 – 1159, Gava Zang, Zanjan, Iran. E-mail: abd@iasbs.ac.ir (H. Abdollahi); Tel.: +98 241 415 3122; Fax: +98 241 415 3232.

1

Abstract

Three-way data obtained from different pulse heights of differential pulse voltammetry (DPV) was analyzed using multivariate curve resolution by alternating least squares (MCR-ALS) algorithm. Differential pulse voltammograms of tryptophan were recorded at a gold nanoparticles decorated multiwalled carbon nanotube modified glassy carbon electrode (GCE/MWCNTs-nanoAu). The determination of tryptophan was performed even in the presence of unexpected electroactive interference(s). Both the simulated and experimental data were non-bilinear. Therefore a Potential shift algorithm was used to correct the observed shift in the data. After correction, the data was augmented and MCR-ALS was applied to the augmented data. A relative error of prediction of less than 8% for the determination of the simulated analyte of interest and tryptophan in synthetic samples indicated that the methodology employing voltammetry and second-order calibration could be applied to complex analytical systems.

2

1. Introduction

More than 30 years ago, Ernest R. Davidson and coworkers at the University of Washington published a five-page report [1] in which they introduced a new concept , second-order advantage, in analytical chemistry. This property, which can commonly be obtained from second-order data allows the quantification of the analyte(s) even in the presence of unexpected sample constituents [2]. Several approaches have been reported for obtaining second order data, such as fluorescence excitation–emission [3], HPLC–DAD [4], LC-ATR-FTIR [5], LC-DAD-MS [6], FIA-DAD [7], DAD-kinetics [8] and pH-DAD [9]. Although these approaches are highly accurate and reliable for the analysis, some of them suffer from several shortcomings such as the high cost of the instrumentation or the complexity of the instrumental method. Therefore, new methods are required for the inexpensive detection and quantification of analytes in a variety of matrices. Electrochemical methods provide good opportunities for accurate and reliable determination of analyte(s) using the low-cost instruments.

Electroanalytical data have been analyzed by many chemometricians during the past four decades. However, during the early development of these methods, the difficulty of the electrochemical hard modeling and the lack of linearity between the current and concentration restricted the application of chemometrics in electroanalytical chemistry [10]. Fortunately, the rapid development of artificial neural networks and dramatic improvements in soft modeling methods, have enhanced the application of chemometrics to electroanalytical data during the last several years [11]. Although several reviews have been published on the different aspects of the application of chemometrics in electroanalytical chemistry [12-16], in these reviews do not cover

3

report of the electrochemical second-order advantage. Recently, two papers [17, 18] have been published in this attractive field. In our previous work we reported the first approach for producing electrochemical second-order data by changing an instrumental parameter (pulse time in DPV). Because we used of an unmodified carbon paste electrode, we could not determine low concentrations of the analyte of interest. Another disadvantage of our previous work was the low sensitivity which was also due to our use of an unmodified electrode [18]. These problems have promted us to use a sensitive sensor for quantifying the analyte of interest in the present work.

Tryptophan (Trp) is one of the essential amino acids which cannot be synthesized by the organism. Therefore it must be supplied in the diet. This compound is a precursor for serotonin (a neurotransmitter), melatonin (a neurohormone), and niacin. It has been implicated as a possible cause of schizophrenia in people who cannot metabolize it properly. The improper metabolization of Trp creates a toxic waste product in the brain that causes hallucinations and delusions [19]

The direct electrochemical oxidation of Trp is known to be kinetically sluggish, and a relatively high overpotential is required for its oxidation at bare electrodes[20]. Electrochemical detection of Trp has been shown to be facilitated by chemically modified electrodes [20-22]. Substantial effort has been devoted to finding new mediators for the fabrication of chemically modified electrodes that can decrease the overpotential of the Trp oxidation. The oxidation peak potential for another electroactive amino acid, tyrosine (Tyr), is very close to that of Trp. Consequently, Tyr is one of the usual interferences in

4

the determination of Trp [23, 24]. Therefore, interest in the development of simple and interference-free methods for the determination of Trp continues.

Nano-structured electrodes, including single electrodes on the nanometer scale and electrodes composed of nano-materials represent new classes of electrodes that can improve the performance of electroanalytical methods [25, 26]. Nano-structured electrodes, in comparison to their bulk counterparts, provide a high effective surface area, enhance mass transport, interact with some biological species efficiently and facilitate their charge transfer. The attachment of metal nanoparticles (NPs) to carbon nanotubes (CNTs), which is often referred as a "decoration" process may lead to the creation of new nano-hybrid materials with the integrated properties of the two components [27]. In addition, these nano-hybrid materials often show interesting properties that are not exhibited by the respective components alone. Therefore, nano-hybrid materials can offer opportunities for the development of new sensors and biosensors with high analytical performance [27].

In the present work, as a part of our research on the applications of chemometrics to the analysis of electrochemical data [18, 28] , we report a simple method based on changes in the pulse height of DPV to create electrochemical second-order data. Because of the non-bilinear behavior of the obtained data, the potential shift correction method is used for the correction of the observed shifts in the data. Then, MCR-ALS is applied on the corrected data to determine the concentration of the analyte. In the present work, a mixture of Trp and Tyr has been chosen as a model for indicating the capability of the method.

5

Finally, the method is employed for the analysis of the electrochemical responses of the new sensor for Trp determination at the gold nanoparticles decorated multiwalled carbon nanotube modified glassy carbon electrode for the determination of Trp in meat extract.

2. Experimental

2.1. Reagents and chemicals

All chemicals were analytical reagent grade and used without further purification. Gold(III) acetate (99.99%) was purchased from Alfa Aesar (Karlsruhe, Germany). Sodium hydroxide, tryptophan, tyrosine and dimethylformamide (DMF) were obtained from Merck (Darmstadt, Germany). Multiwalled carbon nanotubes (MWCNTs, 95% purity, OD = 10-30 nm, ID = 5-10 nm and length = 0.5-500 μm) were obtained from Aldrich (Steinheim, Germany). Double-distilled water was used throughout the experiments..

2.2. Apparatus and software

DPV and cyclic voltammetry (CV) were performed using a Metrohm 746/747 VA and an Autolab potentiostat-galvanostat, model PGSTAT30 (Utrecht, The Netherlands), respectively with a conventional three-electrode set-up. A GCE/MWCNTs-nanoAu, an Ag|AgCl|KCl$_{sat}$ electrode and a platinum wire served as the working, reference and auxiliary electrodes, respectively. Scanning electron microscopy (SEM) was performed with a Philips instrument; model XL-30 (Eindhoven, The Netherlands). A Metrohm 691 pH meter was used for pH measurements. All measurements were performed at room temperature.

Voltammetric data were analyzed in the Matlab environment. MCR-ALS was implemented using the graphical interface provided by Tauler in his web page[29].

6

2.3. Fabrication of GCE/MWCNTs-nanoAu

Au nanoparticles decorated MWCNTs were prepared according to the previously reported method [27]. In brief, the treatment of MWCNTs were treated by refluxing with 70% HNO_3 for 16 h, followed by the filtration and thorough washing of the material with deionized water until pH~7. The acid-treated MWCNTs were dried in a vacuum oven. The pretreated MWCNTs (8 mmol carbon equivalent) were dry mixed with powdered $Au(CH_3COO)_3$ (0.08 mmol) using a mortar and pestle for about 30 min under ambient conditions to prepare AuNPs decorated MWCNTs with a 1 mol % Au loading. The solid, homogenous mixture of $Au(CH_3COO)_3$ and MWCNTs was then transferred to a glass vial, heated under nitrogen in an oven to 300 °C for 1 h and isothermed for 3 h. The product was then collected as the AuNPs decorated MWCNTs (MWCNTs-nanoAu).

The surface of a glassy carbon electrode (GCE) was polished successively with 0.3 and 0.1 μm alumina paste (Struers, Copenhagen, Denmark) to a mirror finish and then cleaned in water under ultrasonication. One milligram of MWCNTs-nanoAu was dispersed in 1 ml DMF with ultrasonic agitation for 1 h to achieve a well-dispersed suspension. Then 2 μL of the prepared MWCNTs-nanoAu suspension was cast onto the surface of the GCE and dried in an oven at 50 °C to prepare a GCE modified with AuNPs decorated MWCNTs (GCE/MWCNTs-nanoAu).

2.4. Preparation of a real sample

A real sample was prepared according to previous reports [30]. The meat sample (250 mg) was dissolved in 3 mL of 4 M sodium hydroxide, sealed in a hydrolysis tube under nitrogen and incubated in an oven at 100 °C for 3 h. The mixture was cooled on an ice bath and neutralized to approximately pH 7 using concentrated HCl. The solution was

7

then diluted to 5 mL with 0.1 M phosphate buffer (pH 7.4). The final solution was filtered through a 0.45 μm filter before the analysis.

3. Results and discussion

3.1. Simulation of non-bilinear second-order data

As previously mentioned, the purpose of this work is to obtain second-order data via a simple change in one of the instrumental parameters of differential pulse voltammetry. In our previous work [18], we demonstrated that a change of the pulse duration(T) in DPV produced a bilinear simulated electrochemical data matrix for an electroactive species. In this work, the pulse height (ΔE) in DPV is changed to obtain electrochemical second-order data. The theory behind the proposed procedure will be briefly discussed.

The current signal intensity in differential pulse voltammetry for a reversible electrochemical reaction can be obtained using equation 1 [31],

$$\delta i = \frac{nFAD_o^{1/2}C_o^*}{\pi^{1/2}(\tau - \tau')^{\frac{1}{2}}} \left[\frac{P_A(1-\sigma^2)}{(\sigma + P_A)(1 + P_A\sigma)} \right] \qquad (1)$$

where

$$P_A = \xi \exp\left[\frac{nF}{RT}(E + \frac{\Delta E}{2} - E^{0'}) \right] \qquad (2)$$

$$\sigma = \exp(\frac{nF}{RT}\frac{\Delta E}{2}) \qquad (3)$$

$\xi = (D_O/D_R)^{1/2}$, ΔE is the pulse height and other symbols have their conventional meanings.

For a typical electrochemical reaction, a data vector can be obtained by sweeping the

8

potential at constant ΔE and τ. Applying a different ΔE and sweeping potential at the constant τ, will produce different data vectors , i.e., sweeping the potential and applying different pulse heights (ΔEs) at a constant pulse duration in DPV produces a non-bilinear second-order data. Then, because of the additive character of the current signal, the second-order data of a two-component mixture can be obtained by adding the current signals of the two components.

For the simulation of a single-component mixture, we supposed that $n = 2$, $F = 96845$ C, $A = 0.2$ cm^2, $D_{o1} = 5\times10^{-6}$ cm^{2}s^{-1}, $C^*_{o1} = 4\times10^{-5}$ M, $R = 8.314$ Jmol^{-1}K^{-1}, $T = 298$ K, $E_{o1} = 0.380$ V, $\tau = 20$ ms and ΔE varies from 20 to 120 mV with a 20 mV increment. For the simulation of a two-component mixture, we simulated the signal matrix of the second species by supposing that $D_{o2} = 6\times10^{-6}$ cm^{2}s^{-1}, $C^*_{o2} = 1.5\times10^{-4}$ M, $E_{o2} = 0.430$ V and other parameters were assumed to be similar to those were used for the first component. Previous reports on the simulation of DPV have confirmed the obtained simulated data [32, 33].

3.2. Analysis of the simulated data

3.2.1. Shift correction

Simulations for a typical reversible system were performed using the supposed values mentioned previously (Fig.1). As it can be seen in the figure 1 by changing the pulse height, the obtained simulated voltammograms shifted and broadened. Shift in peak position for the electrochemically reversible systems happens with changing the pulse height [31]. Similar to that was observed for the simulated data.

A single analyte was considered to be present in the calibration samples of the simulated system (S_1, S_2 and S_3), whereas the interference was included in the test

9

samples (M).

[Figure 1 should be here]

When the obtained data is non-bilinear, the concentration of the analyte of interest can be estimated by non-bilinear rank annihilation (NBRA) [34, 35]. Because of the existence of non-bilinearity in this type of data, a pure component has a rank greater than one. It has been shown that NBRA yields multiple concentration estimates for the analyte of interest. These multiple estimates are usually not identical; some are correct, whereas others are not. Therefore, a concentration estimation of the analyte of interest is confusing. Borgen et al. developed a NBRA method for solving this problem by defining of some concepts such as net analyte rank (NAR) and rank linear additivity (RLA) [36]. Because, the obtained data in this work is full rank, application of Borgen's method for estimation of the analyte of interest seems to be impossible. We therfore, examined other methods for estimating the concentration of the analyte of interest.

MCR-ALS as a powerful chemometrical method and, because it is a good candidate for solving aforementioned problem, was applied on a column-wise augmented data matrix obtained from three standards and one synthetic mixture sample. For the synthetic mixture containing the analyte of interest and the interference, satisfactory results were not obtained by MCR-ALS. The applied constraints in ALS were non-negativity, unimodality (for voltammogram profiles), equality constraint (for the voltammogram profile of the analyte) and selectivity. The lack of linearity in the system produced an excessive lack of fit (lof) of 30%, i.e., convergence was not

10

achieved and the results of MCR-ALS were not satisfactory. The inefficiency of the MCR-ALS model could be due to the potential shift of the data. The shift of potential in the data as a possible source of inefficiency was therefore corrected as described below.

The main premise of multivariate curve resolution (MCR) techniques is to follow the multicomponent Beer's law. Consequently, they can be used to analyze the bilinear data. Appling chemometrics tools such as MCR-ALS to resolve data requires the uniform presentation of data, i.e., all signals have to be adjusted to the same length and corresponding variables have to be placed into the proper columns of the data matrix. The signals obtained from voltammetric techniques often do not fulfill this requirement. This problem is seen as the potential shift in electrochemical data. These facts cause a decrease in the linearity, which depends on the magnitude of the potential shift. In many cases, large lof values as the results of potential shift for MCR-ALS analysis are obtained and impel the analyst to use a higher number of components to explain the non-linearity. Diaz-Cruz et al. recently reported an approach to deal with this problem [10]. They proposed an iterative algorithm in which all the voltammograms were aligned to the same reference position. To correct the potential shift, they used three *Matlab* functions including *peakmaker*, *shiftcalc* and *shiftfit*. *Peakmaker* is a function that generates a Gaussian peak as an initial estimation of the pure voltammograms. The s*hiftcalc* function displaces every signal in every experimental voltammograms matrix for a given potential shift ΔE. The *shiftfit* function iteratively optimizes the values of ΔE to generate a matrix ($\mathbf{I}_{cor}$) in which all signals remain at the fixed potentials stated in the pure voltammograms matrix (V_o) matrix. To perform the potential shift correction, a matrix of the pure

11

voltammograms of the involved electroactive components is required. The pure voltammograms matrix (V_o) was obtained from the simulated data matrix and the *peakmaker* function. The pure voltammogram of the analyte of interest was obtained from the simulated voltammograms of the standard solution of the analyte, and the pure voltammogram of the interference was obtained using the non-bilinear data of the mixture and the *peakmaker* function. Then, the mentioned pure voltammograms were arranged in a matrix to create the pure voltammograms matrix (V_o).

The potential shift correction was performed on a column-wise augmented data matrix that contained three standards of the simulated data matrices of the analyte of interest. All voltammograms of the augmented data were investigated as the pure voltammogram of analyte of interest in the *shiftfit* program. Then, the voltammogram which produced the lowest error in potential shift correction was selected as the pure voltammogram of the analyte of interest. The potential shift correction was also performed on the synthetic mixture (M).

Although the potential shift correction can overcome the non-bilinearity in the data, it produces rank deficient data for the synthetic mixture (M). The synthetic mixture contained two components but the rank of the potential-shift-corrected synthetic matrix was one. Significant results were not achieved for the resolution of this corrected matrix by MCR-ALS. We therefore tried to overcome the rank deficiency problem using matrix augmentation.

3.2.2. Breaking the rank deficiency of corrected data

Matrix augmentation has been reported as a simple and effective approach to the rank

12

deficiency problem [37]. The strategy employed in this work is to augment the rank-deficient signal matrix of the mixture with the potential-shift-corrected data matrices of the standards of the simulated analyte.

Applying MCR-ALS on the augmented data produced a lof of approximately 7%, which was better than that obtained without the potential shift correction. Figure 2 shows the potential shift correction of the augmented data for three simulated standard solutions of the analyte of interest (top left), and one of the synthetic mixtures, M (top right), which have been simulated at a pulse height of 20 to 100 mv with a 20 mv interval. These corrected data were then augmented and standard MCR-ALS was performed on the new augmented data. The results of the potential shift correction and MCR-ALS analysis for the determination of the analyte of interest in the synthetic mixtures (M) are given in Table 1. As evident from the data in the Table, the analysis of the simulated data matrices performed by application of the potential shift correction generates convergence with a much better fit and low lof values. As shown in Table 1, the relative errors of prediction are accepTable; consequently, the proposed method could be efficiently applied for the determination of the analyte in the experimental data.

 [Figure 2 should be here]

3.3. Characterization of GCE/MWCNTs-nanoAu

As shown in figure 1s in supplementary file, the SEM image of MWCNTs-nanoAu powder revealed the formation of Au nanoparticles with diameters of approximately 60 nm on the walls of the carbon nanotubes.

13

Figure 2s shows the cyclic voltammograms of a GCE (a), GCE/MWCNTs(b) and GCE/MWCNTs-nanoAu(c) were recorded in 0.5 M H_2SO_4 solution at a scan rate of 100 mV s^{-1}. The CV of the GCE/MWCNTs-nanoAu showed a typical increase in the anodic peak due to the oxidation of the gold surface on the forward scan (starting at approximately 1.2 V) and its reduction on the reverse scan (at approximately 0.9 V). In addition, the appearance of a pair of oxidation-reduction peaks at approximately 0.4 V is attributed to the quasi-reversible electrochemical behavior of quinone-type carbon oxygen functionalities on the surface of acid-treated MWCNTs, [38] .

3.3.1. Voltammetric characteristics of Trp on GCE/MWCNTs-nanoAu

Preliminary experiments were performed to characterize the behavior of Trp at GCE/MWCNTs-nanoAu. Figure 3 shows the differential pulse voltammograms obtained at GCE (a) in phosphate buffer at pH 7.4 without Trp, and at GCE (b), GCE/MWCNTs (c) and GCE/MWCNTs-nanoAu(d) in the presence of 100 μM Trp. As evident in Fig. 3, the peak potentials of oxidation of Trp at GCE/MWCNTs and GCE/MWCNTs-nanoAu, in comparison with that of GCE, shift approximately 80 and 180 mV, respectively, in the negative direction. In contrast, the peak current of Trp significantly increases after the AuNPs have been decorated on the MWCNTs surface, which indicates the excellent electrocatalytic activity of the MWCNTs-nanoAu hybrid toward Trp oxidation.

 [Figure 3 should be here]

3.3.2. Effect of experimental variables on the anodic peak current of Trp

In the present work, a mixture of Trp and Tyr was chosen as a model mixture to

14

demonstrate the ability of the proposed method. Trp was chosen as the analyte of interest and Tyr was selected as a typical interference in the Trp determination. To select the best conditions for the determination of Trp, the effect of the experimental variables on the peak current of the anodic differential pulse voltammograms of Trp were investigated.

Figure 4A shows the influence of the pH of the Britton-Robinson solution, in the range of 2 to 9, on the current signal intensities of 100 μM Trp. The peak currents did not change significantly up to a pH of 7.4 but decreased significantly at higher pH levels. Thus, a pH of 7.4 for the physiologic buffer was adopted for further studies.

The anodic peak potential of the Trp shifted to more negative values as the pH of the buffer solution was increased (Fig. 4B). The negative shift in the anodic peak potential with increasing pH showed a linear behavior with a slope of -49.9 mV pH^{-1} and an R^2 of 0.9991. This result reveals that the number of protons in the electrochemical reaction is equal to the number of transferred electrons.

The effect of the loading of MWCNTs-nanoAu on the anodic peak current intensity was evaluated by casting different amounts of MWCNTs-nanoAu suspension on the GCE surface (not shown). The amount of MWCNTs-nanoAu on the surface of the electrode is clearly a dominant factor for the oxidation of Trp and for the peak current. The peak current was enhanced by an increase in the amount of MWCNTs-nanoAu and reached a plateau when 2 μL of MWCNTs-nanoAu (1 mg mL^{-1}) was cast. Thus, 2 μL of MWCNTs-nanoAu (1 mg mL^{-1}) was selected for the sensor fabrication.

[Figure 4 should be here]

15

Figure 5 shows the anodic differential pulse voltammograms of Trp (a), Tyr (b) and a mixture of Trp and Tyr (c) at the GCE/MWCNTs-nanoAu under the optimized conditions. As mentioned in the introduction, and as can be observed in Figure 5, the voltammograms of Trp and Tyr exhibit severe overlapping.

[Figure 5 should be here]

3.4. Application of the proposed method for the experimental data

M CR-ALS was performed on a column-wise augmented data matrix obtained from the DPV results of the three standards and a synthetic mixture sample solution. For the synthetic mixture containing Trp and Tyr, satisfactory results were not obtained by MCR-ALS. The applied constraints in ALS were similar to the simulation data. The system's lack of linearity produced an excessive lof of 30%. As previously mentioned, the results of MCR-ALS were not satisfactory because of the presence of potential shifts in the experimental data. Therefore, the potential shift in the data was corrected.

Figure 6 shows the potential shift correction of the augmented data for three standard Trp solutions (top left) and for a synthetic mixture solution containing 40 μM Trp and 80 μM Tyr (top right), which were obtained at a pulse height of 20 to 100 mV with a 20 mV interval. These corrected data were augmented, and MCR-ALS was performed on them. The results of the potential shift correction and the MCR-ALS analysis for the determination of Trp in the synthetic mixtures (M) are given in Table 2. As

16

indicated by the results in Table 2, the analysis of the synthetic data matrices that was performed by application of the potential shift correction generates convergence with a much better fit and low lof values.

[Figure 6 should be here]

3.5. Figure of merit

After decomposition of data matrix by MCR-ALS, the concentration information contained in the concentration profiles can be used for quantitative predictions in a manner similar to that described in ref [9]. In that approach the area under the profile is considered as proportional to component concentration, then the required pseudo-univariate graph is built [9].Then the figure of merit can be obtained by simple calculations for univariate calibration. The sensitivity is the slope of calibration and limit of detection can be calculated as 3s/m.

The calibration plot based on the area under concentration profiles was found to be linear in the $5 - 100$ μM Trp (Y=.0271X + 0.8871 with R^2=9993). Limit of detection was 3 μM of Trp.

3.6. Real sample analysis

We assed the analytical utility of the proposed method was assessed by applying it to the determination of Trp in a fresh meat sample. 1 ml of meat sample extract was added to a volumetric flask and diluted to the mark with the supporting electrolyte (0.1 M phosphate buffer at pH 7.4). Differential pulse voltammograms for the prepared sample solution were recorded (Fig 3s). The potential shift in the real sample data was corrected. The

17

obtained matrix was augmented with the standards matrices, and then MCR-ALS was performed. The results of the Trp determination in the real sample are summarized in Table 3. For a meat extract the amount of Trp was reported in first row of Table 3. In order to evaluate the accuracy of method three spiked samples (rows 3-5 in Table 3) were prepared and recoveries in determination of Trp were calculated. The good recoveries obtained for the spiked samples indicate the successful application of the proposed method for the determination of Trp.

4. Conclusion

The main goals of this work were (I) to create electrochemical second-order data and (II) to perform the analysis in the presence of an unexpected interference. To achieve the first goal, second-order data were created using a simple change in pulse height of differential pulse voltammetry. Because of the non-bilinear behavior of the simulated and experimental data, the potential shift correction algorithm and MCR-ALS were applied to achieve the second goal. Additionally, a gold nanoparticle decorated multiwalled carbon nanotube modified glassy carbon electrode was used as a sensitive sensor was used for the determination of Trp. The proposed sensor exhibited an efficient electrocatalytic activity toward Trp oxidation, which led to a decrease in the overpotential of the process and a remarkable enhancement of the anodic peak current. The proposed method, together with the proposed sensor, was successfully applied for the determination of Trp in a meat sample with satisfactory results. This work proposed the use of a modified electrode to overcome the low sensitivity and high limit of detection that we reported in our previous work. These investigations are the starting point for the production of

18

electrochemical second-order data; future studies in this new field will involve the development of more reliable sensors for electroanalytical determinations.

19

References

[1]   C.N. Ho, G.D. Christian, E.R. Davidson, Anal. Chem., 50 (1978) 1108-13.

[2]   K.S. Booksh, B.R. Kowalski, Anal. Chem., 66 (1994) A782-A91.

[3]   T. Madrakian, A. Afkhami, M. Mohammadnejad, Anal. Chim. Acta, 645 (2009) 25-9.

[4]   Y. Zhang, H.L. Wu, A.L. Xia, Q.J. Han, H. Cui, R.Q. Yu, Talanta, 72 (2007) 926-31.

[5]   A. Edelmann, J. Diewok, J.R. Baena, B. Lendl, Anal. Bioanal. Chem., 376 (2003) 92-7.

[6]   E. Pere-Trepat, R. Tauler, J. Chromatogr. A, 1131 (2006) 85-96.

[7]   A. Checa, R. Oliver, J. Saurina, S. Hernandez-Cassou, Anal. Chim. Acta, 572 (2006) 155-64.

[8]   M.J. Culzoni, P.C. Damiani, A. Garcia-Reiriz, H.C. Goicoechea, A.C. Olivieri, Analyst, 132 (2007) 654-63.

[9]   H.C. Goicoechea, A.C. Olivieri, Appl.Spectrosc., 59 (2005) 926-33.

[10]   A. Alberich, J.M. Diaz-Cruz, C. Arino, M. Esteban, Analyst, 133 (2008) 112-25.

[11]   M. Esteban, C. Arino, J.M. Diaz-Cruz, Crit. Rev. Anal. Chem., 36 (2006) 295-313.

[12]   S.D. Brown, R.S. Bear, Crit. Rev. Anal. Chem., 24 (1993) 99-131.

[13]   Y.N. Ni, S. Kokot, Anal. Chim. Acta, 626 (2008) 130-46.

[14]   M. Esteban, C. Arino, J.M. Diaz-Cruz, Trac-Trend. Anal. Chem., 25 (2006) 86-92.

[15]   V. Pravdova, M. Pravda, G.G. Guilbault, Anal. Lett., 35 (2002) 2389-419.

20

[16]   E. Richards, C. Bessant, S. Saini, Electroanalysis, 14 (2002) 1533-42.

[17]   T. Galeano-Diaz, A. Guiberteau-Cabanillas, A. Espinosa-Mansilla, M.D. Lopez-

Soto, Anal. Chim. Acta, 618 (2008) 131-9.

[18]   H. Abdollahi, M. Kooshki, Electroanalysis, 22 (2010) 2245-53.

[19]. W. Kochen, and H. Steinhart, l-*Tryptophan-Current Prospects in Medicine and Drug Safety*; de-Gruyter: Berlin, 1994.
[20]   S. Shahrokhian, L. Fotouhi, Sensor. Actuators B: Chem., 123 (2007) 942-9.

[21]   K.-J. Huang, C.-X. Xu, W.-Z. Xie, W. Wang, Colloid. Surface. B 74 (2009) 167-

71.

[22]   Y. Guo, S. Guo, Y. Fang, S. Dong, Electrochim. Acta, 55 (2010) 3927-31.

[23]   G.-P. Jin, X.-Q. Lin, Electrochem.Commun., 6 (2004) 454-60.

[24]   F.-H. Wu, G.-C. Zhao, X.-W. Wei, Z.-S. Yang, Microchim. Acta, 144 (2004) 243-

7.

[25]   J.J. Gooding, Electrochim. Acta, 50 (2005) 3049-60.

[26]   P. Bertoncello, R.J. Forster, Biosens. Bioelectron., 24 (2009) 3191-200.

[27]   Y. Lin, K.A. Watson, S. Ghose, J.G. Smith, T.V. Williams, R.E. Crooks, W. Cao,

J.W. Connell, . J. Phys. Chem. C, 113 (2009) 14858-62.

[28]   E. Shams, H. Abdollahi, M. Yekehtaz, R. Hajian, Talanta, 63 (2004) 359-64.

[29]   R. tauler, http://www.ub.es/gesq/mcr/mcr.htm.

[30]   H. Schneider, N. Gerber, B. Friedli-Wunderli, C. Wenk, R. Amado, Mitteilungen

aus Lebensmitteluntersuchung und Hygiene, 97 (2006) 489-98.

[31]   Faulkner.L.R. Bard. A. J, Electrochemical Methods: fundamental and application

2nd ed. Wiley New York, 2001.

 [32]   S.C. Rifkin, D.H. Evans, Anal. Chem., 48 (1976) 2174-9.

21

[33]   J.L. Melville, R.G. Compton, Electroanalysis, 13 (2001) 123-30.

[34]   B.E. Wilson, B.R. Kowalski, Anal. Chem., 61 (1989) 2277-84.

[35]   B.E. Wilson, W. Lindberg, B.R. Kowalski, J. Am. Chem. Soc., 111 (1989) 3797-804.

[36]   Y.D. Wang, O.S. Borgen, B.R. Kowalski, M. Gu, F. Turecek, J. Chemometr., 7 (1993) 117-30.

[37]   A. Izquierdo Ridorsa, J. Saurina, S. HernandezCassou, R. Tauler, Chemometr. Intell. Lab., 38 (1997) 183-96.

[38]   B. Haghighi, S. Bozorgzadeh, L. Gorton, Sensor. Actuators B: Chem., 155 (2011)577.

22

Figures captions:

Figure 1   Simulated DPV second-order data for a typical electroactive species by the proposed method. The pulse heights were 20 to 120 mv with a 20 mv interval

Figure 2: Application of potential shift correction, augmentation of the corrected data, and resolving of the augmented data by MCR-ALS for the simulated data of standards (top left) and the simulated data of a synthetic mixture (top right).

Figure 3: Differential pulse voltammograms obtained at GCE (a) in phosphate buffer solution at pH 7.4 without Trp and at GCE (b), GCE/MWCNTs (c) and GCE/MWCNTs-nanoAu (d) in the presence of 100 μM Trp.

Figure 4: A) Differential pulse voltammograms of 100 μM Trp at a GCE/MWCNTs-nanoAu in Britton–Robinson buffer at different pH levels: a, b, c, d, e, f, g and h were recorded in buffers at pH levels of 1.97, 3.27, 4.02, 5.44, 6.46, 7.35, 8.34 and 9.31, respectively. B) Plot of the peak potential variation with pH; the conditions are the same as in Fig. 4A.

Figure 5: Differential pulse voltammograms obtained for a) a 50 μM Trp solution b) a 50 μM Tyr solution and c) a synthetic mixture containing 50 μM Trp and 50 μM Tyr under the optimized conditions.

Figure 6: Application of potential shift correction, augmentation of the corrected data, and resolution of the augmented data by MCR-ALS for the experimental data of standards (top left) and of a synthetic mixture (top right).

23

Tables captions:

Table 1. MCR-ALS analysis for the determination of the analyte of interest in the simulated unknown samples

Table 2. Results of the potential shift correction and MCR-ALS analysis in the Trp determination in the synthetic samples

Table 3. Results of the analysis of Trp in a real sample using the proposed method

24